MASS LESION DETECTION USING WAVELET DECOMPOSITION TRANSFORM AND SUPPORT VECTOR MACHINE

Ayman AbuBaker

Department of Electrical and Computer Engineering, Applied Science Private University, Amman, Jordan
a_abubaker@asu.edu.jo

ABSTRACT

This paper describes the ongoing efforts by the author to provide efficient and accurate classification for mass lesions in mammogram images. A study of the characteristics of true masses compared to the falsely detected masses is carried out using wavelet decomposition transform combining with support vector machine (SVM). In this approach, four main wavelet features are extracted from different regions of interest in order to distinguish between TP and FP detected regions. A study of detecting regions of interest, extracting the wavelet features and choosing the optimal learning parameters for support vector machine are also presented in this paper. The combined between the wavelet features and SVM presented here can successfully reduces the FP ratio to 0.05 clusters/image, with accurate TP ratio 94%.

KEYWORDS

mammogram, mass lesions, wavelet transform, support vector machine.

1. INTRODUCTION

A Texture analysis has long been an important area in image processing research, where texture is defined [4, 6] as "complex visual patterns composed of entities or sub-patterns that have characteristics brightness, slope, size, etc". Basically, texture analysis aims at segmenting a textured image into disjoint regions each with a uniform texture feature. An effective and efficient texture segmentation method will have many useful applications such as analysis of aerial images, biomedical images and seismic images as well as the automation of certain industrial applications [3]. Texture feature extraction methods can be classified into four categories: structural, statistical, model and transform-based [6]. The structural approaches study the hierarchical structure of texture images and analyze the texture through well defined primitives (micro-textures) and builds a hierarchy of spatial arrangements (macro-textures) based on those primitives [6, 11]. The statistical approaches represent the texture indirectly using the non-deterministic properties that govern the distributions and relationships between the grey levels. Examples include the moments of the gray-level histogram, or statistics based on the gray-level co-occurrence matrix [6]. The model based approach attempts to interpret an image texture using models such as fractal, auto-regression, etc., in order to generate model parameters. These parameters are the keys used to analyze the texture of an image [6, 13]. Finally, the transform based approaches, transform the textured image into the frequency domain before applying texture analysis.

Computerized analysis of mammograms has been investigated in detection the abnormalities in the mammogram images. Many author's techniques are investigated in order to detect the mass lesion in the mammogram images since regarding to the complexity in detecting these regions [8, 9]. Mass detection is a more difficult problem compared to microcalcifications cluster detection because masses are highly connected to the surrounding parenchymal tissue density,

particularly for speculated lesions and they are usually surrounded by non-uniform tissue background with similar characteristics. Usually there are three different sizes for the mass lesion: small size (3–15 mm), middle size (15–30 mm) and large size (30–50 mm) which increases the mass detection complexity [10, 24]. The shape, density and distribution of the mass lesion structure could be described by its texture [5, 25]. To circumvent this issue, a new wavelet decomposition transform method is proposed in this study, based on the fact that one of the abnormal structures which is the mass lesion has a different texture proprieties compared to its neighbour regions. The main purpose for this paper is to study the properties of true positive (TP) and false positive (FP) detected regions in the mammogram images by analyzing their wavelet features and support vector machine (SVM). The combine between wavelet feature and support vector machine (SVM) will be used to reduce number of the detected FP regions. This in turn would help radiologists to improve their performance and save time as they have to go through fewer detected regions.

This paper is organized as follows. A brief survey of previous work is presented in Section 2. A brief description for the used data based is presented in section 3. Where section 4 presents the materials and methods that are used in this proposed approach. The results, discussion and evaluation are presented in Section 5, while concluding remarks are given in Section 6.

2. RELATED WORK

Previous authors have applied various types of techniques to classify the detected mass regions in mammogram images into true positive (TP) and false positive (FP) clusters based on their characteristic features. An automatic contour extraction scheme based on an active contour model (Snakes) to detect the mass lesions in the mammogram images was proposed by Nakagawa et al [14]. In this technique, they first estimate the central point of a mass lesion. Then an initial contour is defined, and a control point's direction of movement is limited to directions radiating from the central point where, the contour was ended in the low contrast level surrounding the mass lesion. Moreover, mass extraction accuracy is increased by choosing the pixel used for processing and using two images, an edge intensity image and a degree of separation image defined based on the concentration histogram, for the calculation of the image forces of a snake. Their evaluation, based on 53 mammogram images, found the algorithm's success in detecting mass lesions ranged from 81% - 100% for 25 cases, ranged from 61% - 80% for 12 cases and was 0% for 16 cases for which it failed detect mass lesions which were present. A local adaptive thresholding filter for detecting mass lesion in mammogram images was proposed by Kom et al. [15]. Their algorithm was based on a design using two concentric widows (inner and outer) in the thresholding process. Their algorithm was evaluated using 61 mammogram images and they achieved 95.91% true positive (TP) detection for the mass lesions with 2 false positive (FP) clusters/image. Qian et al. [16] proposed a new technique for detecting mass lesions using the Ipsilateral Multiview CAD System. In their system, the mediolateral oblique (MLO) and craniocaudal (CC) views were processed using three stages: preprocessing, suspicious regions segmentation, and a concurrent analysis method. In the preprocessing stage, two wavelet-based methods were used for image decomposition and enhancement: a directional wavelet transform (DWT) was used for multiorientation signal decomposition, and a tree structured wavelet transform (TSWT) was designed as an efficient multiresolution enhancement approach. The suspicious region segmentation was carried out using the Fuzzy C-means (FCM) algorithm. Finally, feature extraction and concurrent analysis was carried out in order to classify the suspicious regions into TP or FP regions. Their algorithm achieved on average 89.6% TP with 1 FP cluster/image. Sun et al. [17] modified the ipsilateral multi-view mammograms aiming to improve detection accuracy. They employed nonlinear tree-structured filtering for image noise suppression, two wavelet-based methods, directional wavelet transform and tree-structured wavelet transform for image enhancement, and adaptive fuzzy C-means algorithm for segmentation on each mammogram of the same breast. A

concurrent analysis was developed for iterative analysis of ipsilateral multi-view mammograms by inter-projective feature matching analysis. The modified algorithm achieved 90% TP segmentation of mass lesions with 3 FP clusters/image. Artificial intelligent techniques for the detection of malignant mass lesions were investigated by Cheng et al. [18] who presented a novel fuzzy neural network (FNN) approach. The FNN has four layers: the first is the input layer consisting of 4 fuzzy neurons; the second has 4 ordinary neurons; the third consists of N maximum fuzzy neurons, where N is determined during the training process and varies with the network parameters and data distribution; the fourth has 2 maximum fuzzy neurons and one competitive fuzzy neuron. Texture features were generated using the co-occurrence matrix for Six-hundred and seventy regions manually cropped from 100 mammogram images. They achieved 92% TP detection for mass lesions with 1.33 FP clusters/image. Shih-Chung et al. [22] implemented a multiple circular path convolution neural network (MCPCNN) architecture to detect mass lesions. As a first step, they divided each suspected tumor area into sectors and computed mass features for each sector independently. Then, these sector features were applied to the input layer and were coordinated by convolution kernels of different sizes that propagated signals to the second layer in the neural network system. The best performance obtained for the MCPCNN was 89% TP detection for the mass lesions in the mammogram images. Zheng and Chan [23] presented an algorithm that combines several artificial intelligent techniques with the discrete wavelet transform (DWT) for detection of masses in mammograms. They investigated some AI techniques such as fractal dimension analysis, multi-resolution markov random field, dogs-and-rabbits algorithm, and others to segment the mass lesions. The algorithm was evaluated using 322 mammogram images from MIAS database and was found to segment mass lesions with 97.3% TP with 3.92 FP clusters/image. Zwiggelaar et al. [19] proposed a statistical model-based technique for the detection of two types of speculated lesions, those with linear structures and those with central mass structures. The Principle Component Analysis (PCA) technique models the central mass and the oriented pattern factor analysis technique models the surrounding distorted pattern of the linear structures. The combination of these two techniques provided a complete generic description of speculated lesions in the mammogram images. The algorithm was implemented on a number of mammogram images and detected mass lesions with 80% TP and 0.23 FP clusters/image. Arod´z et al. [20] proposed a pattern recognition method for detecting mass lesions in the mammogram images. The method is based on a two classifier classification scheme, using the AdaBoost and support vector machines (SVM). In the best case the algorithm achieved accuracy of 76% for all lesion types and 90% with 10 % FP for masses only where the SVM based algorithm did not perform well. Eltonsy et al. [21] proposed a morphological model technique to detect the mass lesions in the mammogram images. Their technique is based on the presence of concentric layers surrounding a focal area with suspicious morphological characteristics and low relative incidence in the breast region. The technique was implemented on 270 craniocaudal view cases from the DDSM and achieved 92% TP detection of mass lesions with 5.4 FP clusters/image.

3. DATABASE RESOURCES

In this work, the mass detection algorithm is trained and tested on 70 mammographic images from the University of South Florida (USF) and MIAS databases (40 from USF and the remainder from MIAS). The USF database is a publicly available digital database for mammography screening. Its images are collected from different medical schools and hospitals across the USA. These images all have the same specification (3000 pixel × 4500 pixel and 16-bit pixel depth). This database is divided into four volumes representing the different types of diagnosis: normal, cancer, benign, and benign without call back. Normal images are from patients with normal examination results that have had normal examinations in the previous four years. A normal screening examination is one in which no further "work-up" is required. Cancer images are from patients with screening examinations in which at least one pathology proven cancer is found. Benign cases are from patients with screening examinations in which

something suspicious was found, which turned out to be non-malignant (by pathology, ultrasound or some other means). The term benign without callback is used to identify benign cases in which no additional X-rays or biopsies were done.

The MIAS mammograms have been carefully selected from the United Kingdom National Breast Screening Program. The 322 images represent 161 patients in the MIAS database. These images have been expertly diagnosed and the positions of the MCs and mass lesions in each image are recorded. The mammograms in this database were obtained using the medio-lateral oblique (MLO) view and were digitized at a spatial resolution of 0.05 mm pixel size with 8-bit density resolution. Four image sizes, corresponding to different breast sizes, are included in the 322 images from 161 patients: small (4320 pixel × 1600 pixel), medium (4320 pixel × 2048 pixel), large (4320 pixel × 2600 pixel) and extra large (5200 pixel × 4000 pixel). Digitization was performed on a Joyce-Loeble scanning microdensitometer (SCANDIG-3) which has a linear response in the range 0.0 to 3.2 optical densities.

4. PROPOSED METHOD

This section presents the techniques that are used to detect the mass lesions in the mammogram images. Then the wavelet decomposition transform and SVM are used to reduce the detected FP regions in the mammogram images as shown in Figure 1.
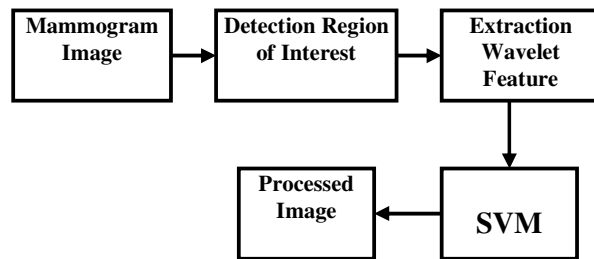

Figure 1. Mass detection flowchart.

4.1. Detection Region of Interest

As a first stage, the regions of interest which includes the mass lesions are detected using the statistical and morphological techniques which are presented in the following subsections.

4.1.1. Peak Detection

Mass lesions appear in digitized mammograms as small to large regions, with intensity values higher than the surrounding region. The maximum size of mass is usually less than 50 mm [12]. Therefore, two concentric masks are used for the initial detections of these regions as shown in Figure 2. When centred on mass lesion, the inner masked region includes the mass lesion while the outer masked region includes the background region.
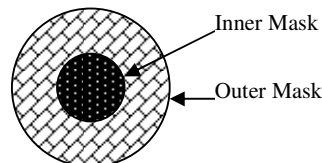

Figure 2. Two concentric masks

The size of the inner mask in pixels is determined by the resolutions of the USF and MIAS databases which are 45 µm × 45 µm and 50 µm × 50 µm respectively. Therefore, the inner mask of size 70 × 70 and outer mask of size 101× 101 are appropriate to initially detect mass regions of size about 50 mm. The average value of the outer masked region, excluding the central region, is used to characterize the surrounding region for comparison with the average value of the inner masked region. So if the average of the inner mask is greater than the value of the average of the outer mask then there is a peak, otherwise it will be ignored.

4.1.2. Thresholding Image and Using Morphological Operator

A global threshold value is set based on the average intensity for the detected peaks. As a result, the output from this method is a binary image where the pixels that have values greater than threshold value are set to 255 and the rest are set to 0 as shown in Figure 3(b).

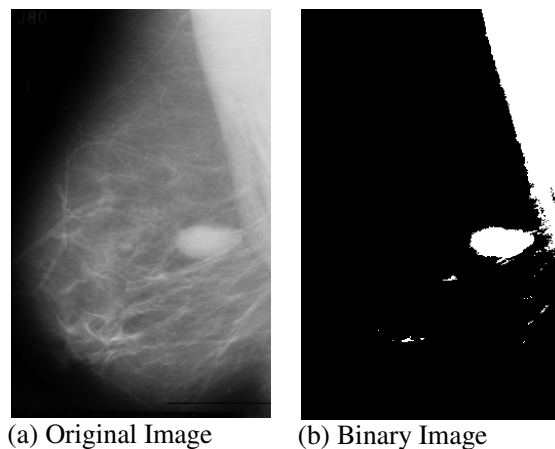(a) Original Image   (b) Binary Image

Figure 3. Mass lesion Threshold

Then, the morphological erosion process is applied in order to remove or reduce the area size the small white region beside separation between the threshold objects. In some cases, the mass lesion is so close to pectoral muscle as in this case, so erosion process is used to separate between these two objects (mass lesion and the pectoral muscle) and at the same time it eliminated small white regions as shown in Figure 4.

Figure 4. Morphological result

4.1.3. Objects Labelling and Size Filter

As illustrated before, the mass lesions have three different sizes, Small, medium and large size. Based on this, the size filter will detect the mass lesion based on the following steps:

1. A novel one scan connected component labelling (OSCCL) algorithm [26] is implemented on the images resulted from the erosion process. The main objective of the OSCCL is to give a unique label for each object in the mammogram image as shown in Figure 5(b). Then the area for each object is computed in pixels.

2. The algorithm tuned so that only masses are preserved after the detection step. Masses of size smaller than 3mm or greater than 30mm not being significant for diagnosis must be left out during detection since the large mass lesion are rarely found in mammogram images [15].Mass lesion has different shapes but the most appropriate size that can include the mass lesion is the circular area. Assuming a circular shape, the maximum area and the minimum area of a mass lesion are identified as 18000 pixel2 and 200 pixel2respectively since the image resolution is 200 micron pixel size which presented by 5 pixels/mm. So, any object exceeded these areas will be set to zero otherwise it will have a value 255 as shown in Figure 5(c).

(a) Thresholded Image   (b) CCL result

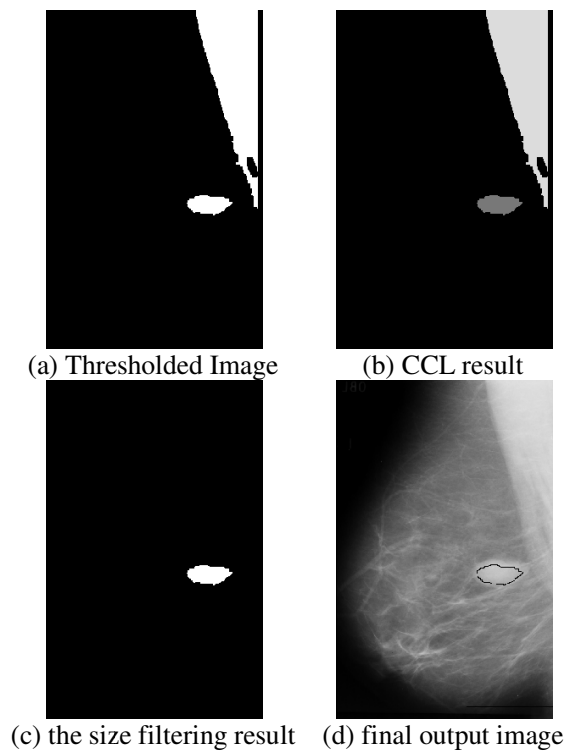(c) the size filtering result   (d) final output image
Figure 5. Processed image

After processing 70 mammogram images, in some mammogram cases the FP regions are appear as shown in Figure 6. Therefore, the extraction wavelet features and SVM are used to remove these FP regions which will be presented in following sections.
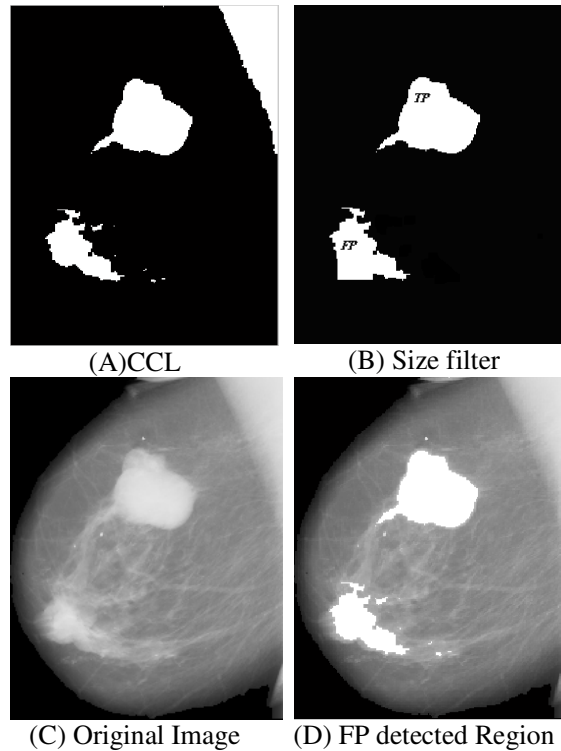
(A)CCL   (B) Size filter

(C) Original Image   (D) FP detected Region
Figure 6. Detected FP region

4.2. Extraction Wavelet Features

In this section, wavelet decomposition is introduced as the main method for feature generation. Due to the nature of mass lesions, which appear as a bright region within a mammogram, they also appear as peak discontinuities for the wavelet transform [29]. This makes the wavelet transform appropriate to detect masses and for feature generation as it is argued that wavelets have finite square supports and are best in capturing point discontinuities and not edges [30].

The Wavelet coefficients are divided into low (L) frequency approximation coefficients and high (H) frequency detail-coefficients. The high frequency coefficients are further divided into detail sub-bands: vertical (LH), horizontal (HL), and diagonal (HH) coefficients. The low frequency (LL) approximation-coefficients provide a reduced resolution representation of the original image which can be transformed again according to the wavelet level applied. Applying wavelet decomposition to an image will produce an approximation matrix that is a quarter of the original area of an image.

Figure 7(A) shows the default view of wavelet decomposition with the features extracted from the top left corner, which is the low frequency image from the second level of decomposition. The results are shown more clearly by changing the default view to the alternative view, Figure 7(B), that shows all the images from each level separately and at the same size. This provides a better view of the differences between levels of decomposition especially when looking at the low frequency image that produces the approximation coefficients for generated features. The figure shows the original image at the top and below it are the approximations from level 1 and level 2 of decomposition showing mass lesion in a larger area than from the original image.

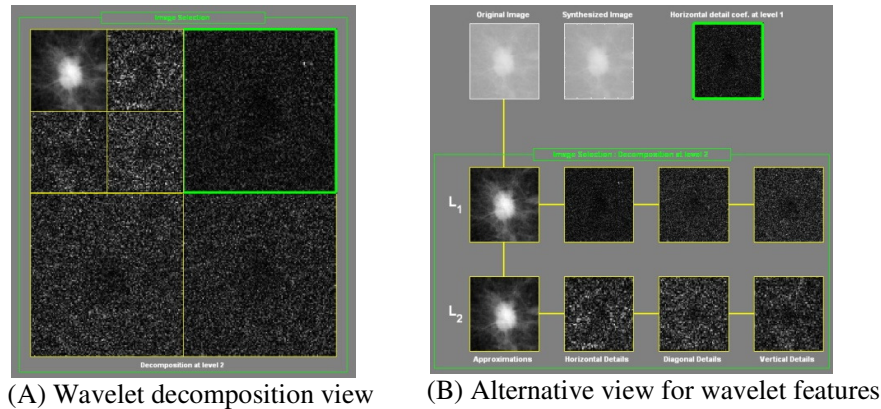(A) Wavelet decomposition view   (B) Alternative view for wavelet features
Figure 7. DB4 decomposition wavelet at level 2

There are many different types of wavelet transforms that can be applied such as Haar, Daubechies, Biorthogonal, Coiflets, Discrete Meyer 'dMey', and Symlets as well as many different ways of defining features. In this paper, the wavelet Daucechies (BD4) transform is used to generate the wavelet coefficient. These coefficients will be used to reduce number of the detected FP regions that are produced in the previous section.

The wavelet DB4 is implemented on the segmented region of interest images of size 70×70 produced by the previous stage. Then, four main features are extracted based on the coefficients of the low frequency image which are maximum value of the coefficients, minimum value of the coefficients, average value of the coefficients, and standard deviation between the coefficients. These features are extracted from low frequency image at each Daucechies (BD4) levels. The maximum DB4 level that is considered in this work is level 3. Therefore, the total number of features for the wavelet Daucechies transform is 12 features for each detected region of interest as shown in the Figure 8.
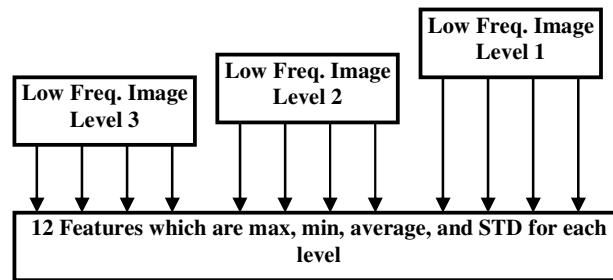

Figure 8. Extraction wavelet features flowchart

Furthermore, in this paper the use of wavelet decomposition to generate features combined with support vector machines for classifications the detected regions produced satisfying results in reducing number of detected FP regions as it will be shown in the next section.

4.2. Classification Process Using SVM

Support Vector Machines (SVM) is a supervised learning technique that can be used for classification and regression [32]. SVMs have a firm statistical foundation and are guaranteed to converge to a global minimum during training. They are also considered to have better generalization capabilities than neural networks [32]. SVMs were developed by Vapnik in [33] based on statistical learning theory. SVM is known to be an excellent tool for binary

classification problems, similar to the one here, by seeking the optimal separating hyperplane that provides efficient separation of the data and maximizes the margin. In other words, SVM takes the closest vectors from both classes, assuming they are linearly separable, and maximizes the distance between them by a hyperplane. On the other hand, if the data are not linearly separable, using kernel functions, SVM will map the data into a higher dimensional feature space where the data can become linearly separable. More information on SVMs can be found in [32] and [33].

Support vector machines are applied in the experiments described in the following sections to evaluate the quality of different feature extraction sets and feature reduction for classification purposes. In this work, there are only two output class labels: normal and abnormal. Hence, the classification is binary.

4.2.1. Data Collection

As SVM is supervised learning technique then the inputs and the outputs data must be known. The inputs data are 12 wavelet features that are extracted from the previous section. Therefore, 120 regions of interest resulted from processing 70 mammogram images. These regions include true positive the false positive regions. As a result, the input matrix includes 12 rows with 120 columns. As the input features are set then the corresponding output class labels, normal and abnormal are generated for each image where the output vector is set to 0.1 and 0.9 for normal and abnormal classes respectively.

4.2.2. Learning Process

The SVM training and testing was carried out based on the statistical Jack-Knife technique [34] in order to have a reliable results. So, the values of the input matrices are arranged in training vectors in a manner similar to the Jackknife technique, where 80% of the inputs data were used for the SVM training phases and the remaining 20% were used for the SVM testing phases.

The SVM learning algorithm used in this work employs the ANOVA kernel technique. The ANOVA kernel technique was adopted because it produced the best classification performance, in a different area of research [32, 33], compared to other types of kernels such as the dot, polynomial, neural and radial kernels. The Anova kernel, which is shown in Eq.(1), has two parameters, the gamma (γ) parameter and the exponential degree (d) parameter. These two parameters control the shape of the kernel.

$$K(x, y) = \left[\sum_i \exp(-\gamma(x_i - y_i)) \right]^d \tag{1}$$

Therefore, different experimental results are implemented to find the optimal value to gamma and the degree as shown in Figure 9.
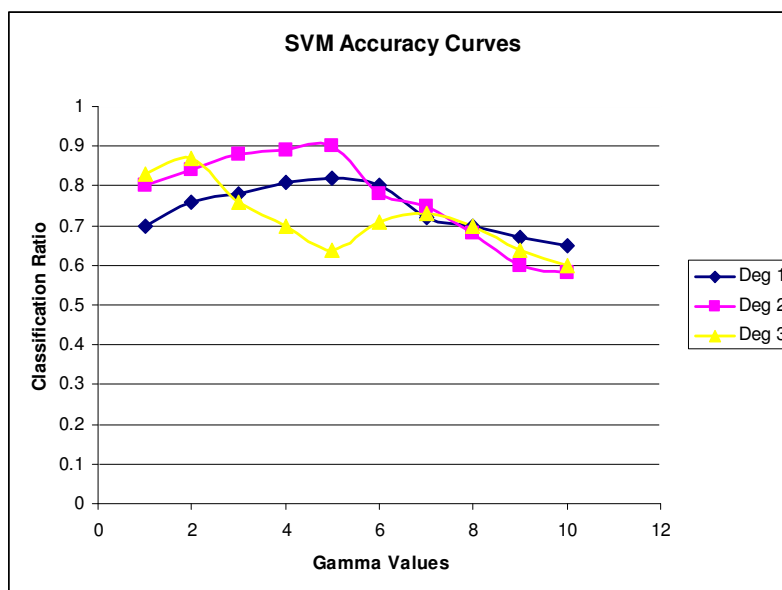
Figure 9. SVM accuracy curves

As shown in the figure above, the optimal value SVM parameters are set as the degree 2 with gamma value 5 with classification ratio 0.9.

5. ALGORITHM EVALUATION

The mass detection algorithm was applied first using 70 mass mammogram images from the USF and MIAS database. The processed images were later subjectively compared with pre-diagnosis cases for the mammogram images from the databases in order to classify the detected regions into TP and FP clusters as shown in Figures 10. Using these classified results, the TP and FP comparisons with other authors was carried out and is shown in Table 1. It is worth mentioning that the TP and FP rates in these authors' publications are reported for different mammogram images and use different benchmarks.

Table 1. The Comparison results using other author's algorithms.

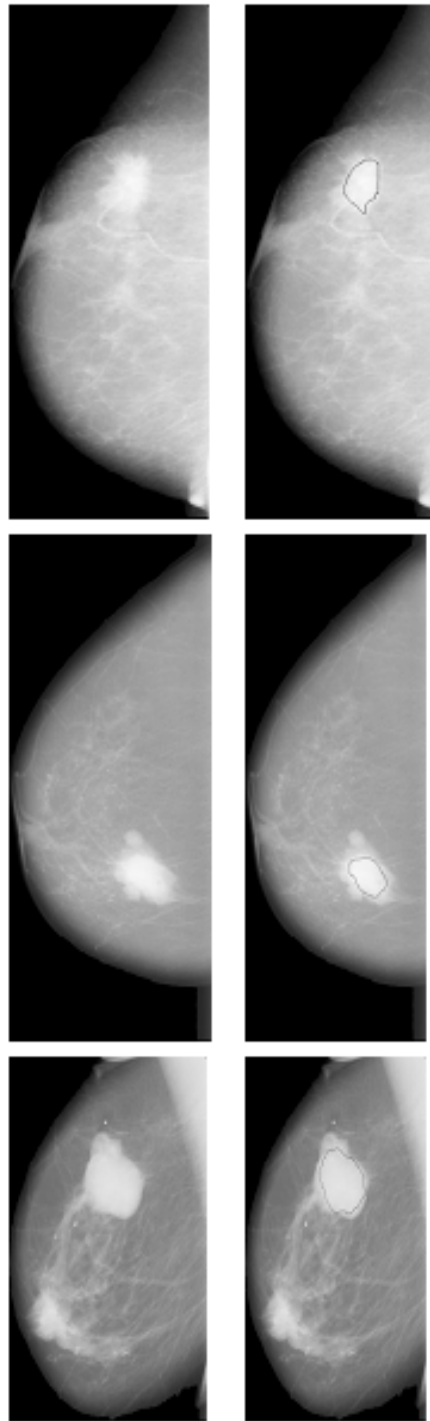| No.	Algorithm	TP	FP
1	Kom et al. [15]	95.91	2 FP/image
2	Qian et al.[16]	89.6	1 FP/image
3	Sun et al. [17]	90	3 FP/image
4	Cheng et al. [18]	92	1.33 FP/image
5	Shih-Chung et al. [22]	89	NA
6	Zheng and Chan [23]	97.3	3.92 FP/image
7	Zwiggelaar et al.[19]	80	0.23 FP/image
8	Arod´z et al. [20]	90	10% FP
9	Eltonsy et al.[21]	92	5.4 FP/image
10	Abubaker [28]	91	0.237 FP/image
11	Proposed Algorithm	93	0.05 FP/image

Figure 10. Accurate Detection of Mass lesions

From table 1, it can be seen that the proposed mass detection algorithm achieves good overall performance compared to other techniques for detected TP and FP regions. The TP percentage achieved for the automatic detection of mass lesions in mammograms from both MIAS and USF databases is about 94 % with a FP rate of about 0.05 clusters/ mammogram.

43

6. CONCLUSIONS

In this paper a novel method for detection the mass lesions in the mammogram images is presented. The proposed method is design using three main stages, detection region of interest, extraction wavelet features, and SVM. In detection region of interest the morphological processing, object labelling, and size filtering are implemented. These steps employ filters designed using the visual characteristics of mass lesions, particularly brightness and size. Then the discrete wavelet transform (DWT) and support vector machines (SVM) with the ANOVA kernel are proposed in reducing the number of the FP regions in the mammogram images. This technique is successfully tested on 70 mass mammogram images with an accuracy detection rate 93% TP with 0.05 clusters/ mammogram FP regions.

REFERENCES

[1] A. A. AbuBaker and R.S.Qahwaji, Musbah J. Aqel, Mohmmad H. Saleh. Mammogram Image Size Reduction Using 16-8 bit Conversion Technique. International Journal of Biomedical Sciences (IJBS), 2006; 1 (2): 103-110.

[2] A. A. AbuBaker, R.S.Qahwaji, Musbah J. Aqel, H. Al-Osta, Mohmmad H. Saleh. Efficient Pre-processing of USF and MIAS Mammogram Images. Journal of Computer Science 2006; 3(2): 67-75.

[3] Hingham R, Brady M. Mammography Image Analysis. Kluwer Academic Publishers, 1999.

[4] Daniel B, Md Kopans. Breast Imaging. Lippincot Williams, 1997.

[5] Karssemeijer N and te Brake G. Detection of stellate distortions in mammogram. IEEE Trans. on Medical Imaging, 1996; 15(5): 611-619.

[6] Materka, M. Strzelecki. Texture Analysis Methods – A Review. Technical University of Lodz, Institute of Electronics, COST B11 report, Brussels 1998.

[7] Ayman AbuBaker, Rami Qahwaji and Stan Ipson. Knowledge-based Approach to the Automatic Detection of Microcalcifications in Mammogram Images. Submitted to the Journal of Medical Image Analysis, 2007.

[8] L.W. Bassett, D.H. Bunnell, R.H. Gold, R.D. Arndt, J. Linsman, Breast cancer detection: one versus two views, Radiolgy 165, 1987,pp. 95–97.

[9] D. Wolerton, R.M. Nishikawa, W. Zouras, K. Doi, CAD in digital mammography: computerized detection and classification of masses, in: A.G. Gale et al. (Eds.), Digital Mammography, Elsevier Science BV, Amsterdam, 1994.

[10] H. Li, Y. Wang, K.J. Ray Liu, B.L. Shih-Chung, M.T. Freedman, Computerized radiographic mass detection. Part II: decision support by featured database visualization and modular neural networks, IEEE. Trans. Med. Imag. 20 (4) ,2001,pp. 302–313.

[11] K. Bovis, S. Singh, J. Fieldsend, C. Pinder, Identification of masses in digital mammograms with MLP and RBF nets, in: Proceedings of the IEEE-INNS-ENNS International Joint Conference on Neural Networks Com, 2000, pp. 342–347.

[12] P. Skaane, K. Engedal, A. Skjennald, Interobserver variation in the interpretation of breast imaging, Acta Radiol. 38, 1997, pp. 497–502.

[13] H. Li, Y. Wang, K.J. R Liu, S.B. Lo, M.T. Freedman, Computerized radiographic mass detection— Part I: lesion site selection by morphological enhancement and contextual segmentation, IEEE Trans. Med. Imaging 20, 2001,pp. 289–301.

[14] T. Nakagawaa, T. Harab, H. Fujitab, T. Iwasec, T. Endod, K. Horita, Automated contour extraction of mammographic mass shadow using an improved active contour model, International Congress Series 1268, 2004, pp. 882–885.

[15] Guillaume Kom, Alain Tiedeu, Martin Kom, Automated detection of masses in mammograms by local adaptive thresholding, Computers in Biology and Medicine 37, 2007,pp. 37 – 48.

[16] Wei Qian, Dansheng Song, Minshan Lei, Ravi Sankar, Edward Eikman, Computer-Aided Mass Detection Based on Ipsilateral Multiview Mammograms, Acad Radiol, 2007, 14: 530–538

[17] Xuejun Sun, Wei Qian, Dansheng Song, Ipsilateral-mammogram computer-aided detection of breast cancer, Computerized Medical Imaging and Graphics 28, 2004,pp. 151–158

[18] H.D. Cheng, Muyi Cui, Mass lesion detection with a fuzzy neural network, Pattern Recognition 37, 2004,pp. 1189 – 1200

[19] Reyer Zwiggelaar, Timothy C. Parr, James E. Schumm, Ian W. Hutt, Christopher J. Taylor, Susan M. Astley and Caroline R. M. Boggis, Model-based detection of speculated lesions in mammograms, Medical Image Analysis, volume 3, number 1, 1999,pp 39–62

[20] Tomasz Arod´z, Marcin Kurdziel, Erik O.D. Sevreb, David A. Yuenb, Pattern recognition techniques for automatic detection of suspicious-looking anomalies in Mammograms, Computer Methods and Programs in Biomedicine 79, 2005,pp.135—149.

[21] Nevine H. Eltonsy, Georgia D. Tourassi, and Adel S. Elmaghraby, A Concentric Morphology Model for the Detection of Masses in Mammography, IEEE TRANSACTIONS ON MEDICAL IMAGING, VOL. 26, NO. 06, JUNE 2007.

[22] Shih-Chung B. Lo, Huai Li, Yue Wang, Lisa Kinnard, and Matthew T. Freedman, A Multiple Circular Path Convolution Neural Network System for Detection of Mammographic Masses, IEEE TRANSACTIONS ON MEDICAL IMAGING, VOL. 21, NO. 2, FEBRUARY 2002.

[23] Lei Zheng and Andrew K. Chan, An Artificial Intelligent Algorithm for Tumor Detection in Screening Mammogram, IEEE TRANSACTIONS ON MEDICAL IMAGING, VOL. 20, NO. 7, JULY 2001

[24] A. A. AbuBaker and R.S.Qahwaji, Musbah J. Aqel, Mohmmad H. Saleh" Mammogram Image Size Reduction Using 16-8 bit Conversion Technique" International Journal of Biomedical Sciences (IJBS), 1 (2): PP. 103-110, 2006.

[25] AbuBaker, A. A., Qahwaji, R.S., Ipson, S. S., Mammogram Image Segmentation Using Statistical and Morphological based Techniques, 8th informatics workshop, University of Bradford, 2007, pp.8-11.

[26] A. A. AbuBaker, R.S.Qahwaji, Stan Ipson, Mohmmad H. Saleh, "One Scan Connected Component Labelling Technique", IEEE International Conference on Signal Processing and Communication, Dubai, United Arab Emirates, 2007, pp. 1283-1286.

[27] A. AbuBaker: Automatic Detection of Breast Cancer Microcalcifications in Digitized X-ray Mammograms, Ph.D. Thesis, School of Informatics, University of Bradford-UK, 2008.

[28] Ayman,AbuBaker, Rami, Qahwaji, Stan, Ipson. *Mass Lesion Detection Using Statistical and Morphological Techniques*, pp. 116-112, 7th IEEE International Conference on Cybernetic Intelligent Systems, 2008.

[29] Sampat, M.P., Markey, M.K., and Bovik, A.C., Computer-aided detection and diagnosis in mammography, in Handbook of Image and Video Processing, 2nd ed. 2005, New York: Academic Press. pp. 1195-1217.

[30] Ferreira, C.B. and Borges, D.L., Automated mammogram classification using a multiresolution pattern recognition approach. Proc. XIV Brazilian Symposium on Computer Graphics and Image Processing, 2001: pp. pp. 76- 83.

[31] Sewell, M. Support Vector Machines (SVMs). [cited 2009 February]; Available from: http://www.svms.org.

[32] Qahwaji, R. and Colak, T., Automatic Short-Term Solar Flare Predection Using Machine Learning and Sunspot Associations. Solar Physics, 2007. 241(1): pp. 195-211.

[33] Vapnik, V., The Nature of Statistical Learning Theory. Springer Verlag. 1999, New York.

[34] K. Fukanga, Introduction to Statistical Pattern Recognition. San Diego, CA: Academic, 1990.

[35] G. Eason, B. Noble, and I. N. Sneddon, "On certain integrals of Lipschitz-Hankel type involving products of Bessel functions," Phil. Trans. Roy. Soc. London, vol. A247, pp. 529–551, April 1955. *(references)*

[36] J. Clerk Maxwell, A Treatise on Electricity and Magnetism, 3rd ed., vol. 2. Oxford: Clarendon, 1892, pp.68–73.

[37] I. S. Jacobs and C. P. Bean, "Fine particles, thin films and exchange anisotropy," in Magnetism, vol. III, G. T. Rado and H. Suhl, Eds. New York: Academic, 1963, pp. 271–350.

[38] K. Elissa, "Title of paper if known," unpublished.

[39] R. Nicole, "Title of paper with only first word capitalized," J. Name Stand. Abbrev., in press.

[40] Y. Yorozu, M. Hirano, K. Oka, and Y. Tagawa, "Electron spectroscopy studies on magneto-optical media and plastic substrate interface," IEEE Transl. J. Magn. Japan, vol. 2, pp. 740–741, August 1987 [Digests 9th Annual Conf. Magnetics Japan, p. 301, 1982].

[41] M. Young, The Technical Writer's Handbook. Mill Valley, CA: University Science, 1989.

Author

Ayman Abubaker: he got his B.Sc. in Electrical Engineering on 1999. On 2008 he finished his PhD in Electronic Imaging and Media Communications (EIMC) from School of Informatics, University of Bradford- UK. His main research focused on processing medical images such as mammogram images (detecting microcalcifications and mass lesions), ultrasound images and MRI images. He is currently assistance professor at Electrical and Computer Engineering Dept., Applied Science Private University, Amman-Jordan.